Dopaminergic dysfunction in unrelated, asymptomatic carriers of a single parkin mutation

To the Editor: We read with interest the article by Khan et al.[1] The authors studied asymptomatic parkin heterozygotes by 18F-dopa PET and found a significant reduction of uptake in putamen, caudate, dorsal and ventral midbrain. An interesting observation relates to the subtle extrapyramidal symptoms in four of these "asymptomatic" carriers. The authors recommended follow-up to verify whether they develop parkin disease.

One of our patients with a single parkin mutation developed parkin disease 23 years after the manifestation of tremor as the only symptom. This 56-year-old man is the only child of nonconsanguineous parents of European Jewish origin. At age 13, left hand tremor was noticed. Tremor severity remained unchanged for 23 years (without treatment), until the age of 36, when he experienced prominent rest tremor and bradykinesia of the left limbs.

Five years later, L-dopa was initiated with excellent response. Dyskinesias occurred 3 years after L-dopa onset, necessitating a left pallidotomy 18 years later. Brain MRI was normal. Genetic testing revealed a heterozygous C to T transition at nucleotide position 1197 of parkin gene (exon 10).

Parkin disease presents as slowly progressive parkinsonism.[2,3] Even if significant dopaminergic dysfunction appears in PET studies of single parkin mutation carriers, other mechanisms and the amount of intact dopamine store at a young age might be compensatory to prevent early clinical expression.[1]

However, this explanation may only relate to some patients. Others might develop parkin disease earlier, as occurred in another of our sporadic patients who carries a single parkin mutation. This 36-year-old woman is the only child of nonconsanguineous parents of European Jewish origin. At the age of 31, she experienced left foot dystonia, slowing of her left hand accompanied by rest tremor, which later progressed to bilateral parkinsonism. Response to L-dopa given 5 years after disease onset was excellent. Brain MRI was normal. A heterozygous deletion of exon 7 of parkin was found.[4]

Haploinsufficiency (reduction in normal protein function) and dominant negative effects (nonfunctional polypeptide physically interferes with normal protein) proposed as causes of dopaminergic cell dysfunction[1] or the inhibition of parkin's ubiquitin 3 ligase activity by S-nitrosylation[5] are probably not the only explanations. Other genetic or environmental factors might predispose carriers of a single parkin mutation not only to late-onset but also to young-onset Parkinson disease.

Rivka Inzelberg, MD, Nobutaka Hattori, MD, Yoshikuni Mizuno, MD, *Hadera, Israel*

Editor's Note: The authors had the opportunity to respond to this Correspondence but declined.

References

1. Khan NL, Scherfler C, Graham E, et al. Dopaminergic dysfunction in unrelated, asymptomatic carriers of a single parkin mutation. Neurology 2005;64:134–136.
2. Nisipeanu P, Inzelberg R, Abo Mouch S, et al. Parkin gene causing benign autosomal recessive juvenile parkinsonism. Neurology 2001;56:1573–1576.
3. Inzelberg R, Hattori N, Nisipeanu P, et al. Camptocormia, axial dystonia, and parkinsonism: Phenotypic heterogeneity of a parkin mutation. Neurology 2003;60:1393–1394.
4. Inzelberg R, Nisipeanu P, Carasso RL, Blumen SC, Hattori N, Mizuno Y. Early-onset parkinsonism in heterozygous parkin mutation carriers. Ann Neurol 2004;56(suppl 8):S28.
5. Choung KKK, Thomas B, Li X, et al. S-nitrosylation of parkin regulates ubiquitination and compromises parkin's protective function. Science 2004;304:1328–1331.

fMRI reveals large-scale network activation in minimally conscious patients

To the Editor: We read Schiff et al.'s article with great interest.[1] We conducted a case study regarding the application of fMRI to a patient in a minimally conscious state.[2] The Schiff et al. article appears to corroborate our findings of multisensory and cognitive fMRI BOLD responses in an overtly unresponsive brain-injured patient. These initial reports probing the minimally conscious state with imaging methods offer intriguing possibilities, and indeed the 2001 fMRI case study closely correlated with the patient's eventual recovery. Further research in this area is warranted.

Chad H. Moritz, PhD, *Madison, WI*

To the Editor: Schiff et al.[1] reported that two severely brain-injured patients monitored with fMRI showed brain responses to auditory personal narratives but not when the input was presented in reverse, meaningless form. A similar study[3] with equally remarkable results was carried out more than 20 years earlier, ironically also by researchers at Columbia University. That it was overlooked by Schiff et al. is an indication of the obscurity into which this study has undeservedly fallen.

In the earlier report of Boyle and Greer, three brain-injured patients with disabilities at least as severe as those in the Schiff et al. study were examined. In place of monitoring by fMRI, operant conditioning was used to increase small spontaneous responses made by each patient including eyelid, finger, or mouth movements. The reinforcer in each case was the playing of a 15-second sample of music identified as the patient's favorite, presented contingent on an occurrence of the target response. A multiple-baseline design with reversal,[4] a technique of the field of applied behavior analysis, was used to assess causal relationships. The authors reported good evidence of learning for the first patient, lesser but suggestive evidence for the second, and little evidence of learning for the third.

The first patient subsequently recovered from the vegetative state to a limited extent, the second did not recover, and the third died within 1 week after the end of testing. Thus successful operant conditioning may possibly predict recovery and may even help produce it.

Schiff et al. concluded in their later study that their findings of changes in brain activity in response to meaningful auditory input "raise important questions related to whether MCS [minimally conscious state] patients have a greater capacity to experience subjective states but also to benefit from therapeutic intervention." The results of the Boyle and Greer study raise the same questions, but go one step further by showing an actual change in behavior in response to reinforcement by emotionally meaningful stimuli.

Although the methods differ, the results of the two studies complement each other. Both methods should be exploited as valuable tools towards the goals of understanding and enhancing the capabilities of the brain-injured, minimally conscious patient.

Stephen L. Black, PhD, *Lennoxville, Canada*

Editor's Note: The authors had the opportunity to respond but declined.

References

1. Schiff ND, Rodriguez-Moreno D, Kamal A, et al. fMRI reveals large-scale network activation in minimally conscious patients. Neurology 2005;64:514–523.
2. Moritz CH, Rowley HA, Haughton VM, Swartz KR, Jones J, Badie B. Functional MR imaging assessment of a non-responsive brain injured patient. Magn Reson Imaging 2001;19:1129–1132.
3. Boyle ME, Greer, RD. Operant procedures and the comatose patient. J Appl Behav Anal 1983;16:3–12.
4. Kazdin A. Behavior Modification in Applied Settings, 6th ed. Belmont, CA: Wadsworth; 2001.

Preserved Cardiac Sympathetic Nerve Accounts for Normal Cardiac Uptake of MIBG in PARK2

Satoshi Orimo, MD, PhD,[1]* Takeshi Amino, MD,[1] Masayuki Yokochi, MD, PhD,[2] Tohru Kojo, MD, PhD,[3] Toshiki Uchihara, MD, PhD,[3] Atsushi Takahashi, MD, PhD,[4] Koichi Wakabayashi, MD, PhD,[5] Hitoshi Takahashi, MD, PhD,[6] Nobutaka Hattori, MD, PhD,[7] and Yoshikuni Mizuno, MD, PhD[7]

[1]Department of Neurology, Kanto Central Hospital, Tokyo, Japan; [2]Department of Neurology, Ebara Metropolitan Hospital, Tokyo, Japan; [3]Department of Neuropathology, Tokyo Metropolitan Institute for Neuroscience, Tokyo, Japan; [4]Organ and Function Pathology Division, Yokufukai Geriatric Hospital, Tokyo, Japan; [5]Department of Neuropathology, Hirosaki University School of Medicine, Hirosaki, Japan; [6]Department of Pathology, Brain Research Institute, University of Niigata, Niigata, Japan; [7]Department of Neurology, Juntendo University School of Medicine, Tokyo, Japan

Abstract: **We performed [^{123}I] MIBG myocardial scintigraphy in two of three patients with PARK2 from unrelated families and examined the heart tissues from the three patients immunohistochemically using an antibody against tyrosine hydroxylase (TH) to see whether cardiac sympathetic nerve is involved. Cardiac uptake of MIBG was normal except for a slight decrease in the late phase in one of the patients. Postmortem examination revealed that TH-immunoreactive nerve fibers in the epicardium were well preserved in all three patients. The present study confirmed that cardiac sympathetic nerve is well preserved in PARK2 with a homozygous exon deletion, which accounts for normal cardiac uptake of MIBG. Moreover, normal cardiac uptake of MIBG might be of potential diagnostic value to indicate the absence of Lewy body pathology, even in patients with levodopa-responsive Parkinsonism, as in PARK2.**

Key words: PARK2; Parkinson's disease; MIBG myocardial scintigraphy; cardiac sympathetic nerve; denervation

*Correspondence to: Dr. Satoshi Orimo, Department of Neurology, Kanto Central Hospital, 6-25-1 Kami-Yoga, Setagaya-ku, 158-8531 Tokyo, Japan. E-mail: orimo@kanto-ctr-hsp.com

Received 24 December 2004; Revised 27 January 2005; Accepted 31 January 2005

Published online 6 July 2005 in Wiley InterScience (www.interscience.wiley.com). DOI: 10.1002/mds.20594

PARK2 is an autosomal recessive inherited form of familial Parkinsonism caused by mutations of *parkin*,[1] a gene that maps to chromosome 6q25-q27,[2] and is characterized by early onset of the disease usually before the age of 40 years, dystonia, hyperreflexia, sleep benefit, early complications from levodopa treatment, and slow progression.[3] Neuropathological findings of PARK2 are characterized by generalized loss of neurons in the substantia nigra pars compacta and locus coeruleus with no Lewy bodies.[4–6] PARK2 can be differentiated from idiopathic Parkinson's disease (PD) by means of early onset of the disease and other characteristics described above. However, it is sometimes difficult to differentiate PD from PARK2, because some patients with PARK2 develop clinical features after the age of 40 years.[7,8]

Decreased cardiac uptake of *meta*-iodobenzylguanidine (MIBG) on [^{123}I] MIBG myocardial scintigraphy, which indicates cardiac sympathetic denervation, has been reported in patients with PD. This imaging approach might be a new diagnostic tool to differentiate PD from other movement disorders with similar symptomatology such as multiple system atrophy (MSA), progressive supranuclear palsy (PSP), and corticobasal degeneration (CBD).[9–13] Cardiac sympathetic denervation in PD was also reported by means of decreased cardiac uptake of 6-[^{18}F] fluorodopamine on positron emission tomography.[14] Recently, we reported depletion of cardiac sympathetic nerve in patients with PD but not in patients with MSA, which accounted for the difference in cardiac uptake of MIBG between PD and MSA.[15,16] In contrast, cardiac uptake of MIBG has been reported to be normal in patients with autosomal recessive juvenile Parkinsonism[17] and a single patient with PARK2.[18] Therefore, [^{123}I] MIBG myocardial scintigraphy might be a useful diagnostic tool to differentiate PARK2 from PD.

In the present report, we studied three genetically and pathologically confirmed patients with PARK2 from unrelated families to see whether cardiac sympathetic nerve was involved by means of [^{123}I] MIBG myocardial scintigraphy and pathological examination.

PATIENTS AND METHODS

Patient 1

A 73-year-old man with PARK2 with a homozygous exon 4 deletion in the *parkin* gene developed a tremor in both hands at the age of 24, followed by gait disturbance. These features responded well to levodopa. He had no autonomic symptoms, and he had no signs such as orthostatic hypotension (OH), severe constipation, and frequency of urination. His parents were consanguineous and his younger brother and two younger sisters had been diagnosed as having PARK2. A single photon computed tomography (SPECT) of [^{123}I] MIBG myocardial scintigraphy at the age of 70, 46 years after the onset, showed normal cardiac uptake of MIBG in both the early (Fig. 1A) and the late phase. Heart-to-mediastinum (H/M) ratio of the early and late phase was 2.28 and 2.30, respectively. That of the early and late phase of age-matched control (8 men and 6 women; 59–81; 71.9 ± 6.6 years of age) was 2.20 ± 0.15 and 2.14 ± 0.19, respectively. Postmortem examination 3 hr after death revealed loss of pigmented neurons and gliosis in the substantia nigra pars compacta and locus coeruleus with no Lewy body pathology.

Patient 2

A 66-year-old man with PARK2 with a homozygous exon 4 deletion in the *parkin* gene developed a tremor, rigidity, and gait disturbance at the age of 28. These features responded well to levodopa. He had no autonomic symptoms or signs. He had hypertension with no antihypertensive medications. A SPECT of [^{123}I] MIBG myocardial scintigraphy at the age of 63 years, 35 years after the onset, showed normal cardiac uptake of MIBG in the early phase (Fig. 1B) and a slight decrease in the late phase. H/M ratio of the early and the late phase was 1.98 and 1.69, respectively. Postmortem examination 2 hr after death revealed loss of pigmented neurons and gliosis in the substantia nigra pars compacta and locus coeruleus with no Lewy body pathology. The weight of the heart was 400 gm and a histological examination was unremarkable.

Patient 3

A 70-year-old man with PARK2 with a homozygous exon 4 deletion in the *parkin* gene had been reported clinically and neuropathologically elsewhere.[6] Briefly, he developed a dystonic gait at the age of 32, followed by hand tremor, rigidity, bradykinesia, and postural instability. These features responded well to levodopa. He had no OH but had constipation and frequency of urination 2 years before his death. Postmortem examination 4 hr after death revealed loss of pigmented neurons and gliosis in the substantia nigra pars compacta and locus coeruleus with no Lewy body pathology.

Methods

We immunohistochemically examined the heart tissues using an antibody against tyrosine hydroxylase (TH), a rate-limiting enzyme of catecholamine biosynthesis. The anterior wall of the left ventricle of the heart was selected based on previous studies[15,16] because TH-immunoreactive nerve fibers were more numerous in the anterior than in the posterior wall of the ventricle[19] and cardiac uptake of MIBG is mainly observed in the left ventricle. The blocks from Patients 1, 2, and 3 and three patients with neuropathologically confirmed Lewy body pathology-positive PD as well as three control subjects (Table 1) were fixed with formalin and embedded in paraffin. Deparaffinized sections were stained with hematoxylin and eosin (H&E) or immunostained with a monoclonal antibody against TH (Sigma, St. Louis, MO; dilution 1:5,000) by the avidin–biotin–peroxidase complex method with Vectastain kit (Vector, Burlingame, CA). The peroxidase labeling was visualized with diaminobenzidine-nickel as chromogen. The number of TH-immunoreactive nerve fibers in the epicardium was assessed according to a semiquantitative rating scale: −, absent or nearly absent; +, sparse; ++, moderate; +++, numerous.

RESULTS

The clinical characteristics and TH immunopositivity are shown in Table 1. On routine HE staining, no abnormal findings were found in either the myocardium or the epicardium of each patient and control subjects. There were moderate to numerous TH-immunoreactive nerve fibers in the epicardium from all the patients with PARK2 (Fig. 2A–C, Table 1) as well as from control subjects (Fig. 2E, Table 1). In contrast, the number of TH-immunoreactive nerve fibers was absent or nearly absent in the epicardium from all the patients with PD (Fig. 2D, Table 1).

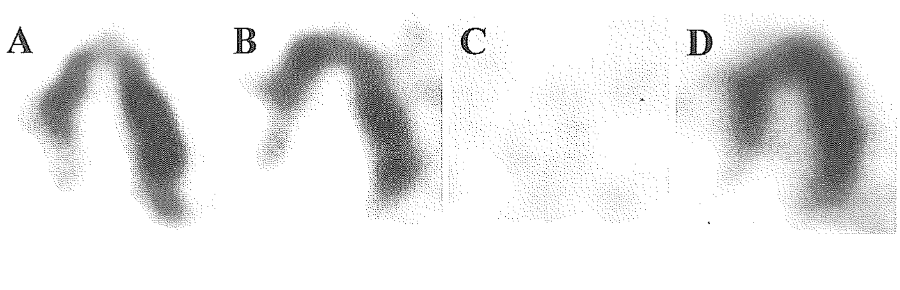

FIG. 1. Long axis of SPECT images of two patients with PARK2, a patient with PD (67 years of age; female; duration of illness, 3 years) and a control subject (64 years of age; female). Cardiac uptake of MIBG of the patients with PARK2 is normal (**A** and **B**) as well as that of the control subject (**D**). In contrast, that of the patient with PD is severely decreased (**C**).

TABLE 1. *Clinical characteristics, H/M ratio, and TH immunopositivity*

Patient	Diagnosis	Age (yr)	Sex	Duration (yr)	Type of mutation (deletion)	H/M (early)	TH
1	PARK2	73	M	49	Exon 4	2.28	++~+++
2	PARK2	66	M	38	Exon 4	1.98	+++
3	PARK2	70	M	38	Exon 4		++~+++
4	PD	70	M	10			−
5	PD	82	F	10			−
6	PD	91	F	15			−
C1	Peritonitis	81	F				+++
C2	Colon cancer	86	M				+++
C3	Esophageal cancer	89	F				+++

TH, tyrosine hydroxylase; PD, Parkinson's disease.

DISCUSSION

The present patients had typical PARK2 clinical characteristics such as early onset, effectiveness of levodopa treatment, and long duration of illness. Autonomic symptoms and signs were absent or very mild in all the patients. They all had the *parkin* gene mutation, a homozygous exon 4 deletion, and were diagnosed as having PARK2.

Decreased cardiac uptake of MIBG or fluorodopamine in PD has been reported.[9–14] Cardiac uptake of fluorodopamine is also decreased in patients with familial Parkinsonism as seen in PARK1 (linked to a mutant form of α-synuclein) or in PARK4 (overproduction of normal α-synuclein) patients, who have OH and Lewy body pathology.[20] Our patients with PARK2, who have neither OH nor Lewy body pathology, showed normal cardiac uptake of MIBG except for a slight decrease in the late phase in one of the patients, in spite of the fact that the duration of this patient's was over 30 years. Although this slight decrease in the late phase may represent early involvement of cardiac sympathetic nerve,[10,12] it is attributable to increased exocytosis due to hypertensive heart disease.[21] The present findings and a previous report,[18] even considering the limited number of patients, strongly suggest that cardiac uptake of MIBG is a useful diagnostic marker to differentiate PARK2 from PD. Moreover, the present findings indicate that normal cardiac uptake of MIBG is associated with the absence of Lewy body pathology and that, in turn, the decease in cardiac uptake of MIBG is closely related to the presence of Lewy body pathology. This assumption is further supported by well-preserved TH-immunoreactive nerve fibers, which is presumably cardiac sympathetic nerve,[16] in the epicardium of our three patients with PARK2. This is in sharp contrast with patients with PD, who have decreased cardiac uptake of MIBG, depletion of cardiac sympathetic nerve, and Lewy body pathology. It might be worth mentioning that patients with familial Parkinsonism caused by inherited α-synucleinopathies had OH from sympathetic failure, whereas none of the patients with PARK2 had OH. This finding provides indirect support for a contribution of sympathetic denervation to OH in PD.

In conclusion, the present study confirmed that cardiac sympathetic nerve is well preserved in PARK2 with homozygous exon deletion, which accounts for normal cardiac uptake of MIBG. Moreover, normal cardiac uptake of MIBG might be of potential diagnostic value to indicate the absence of Lewy body pathology.

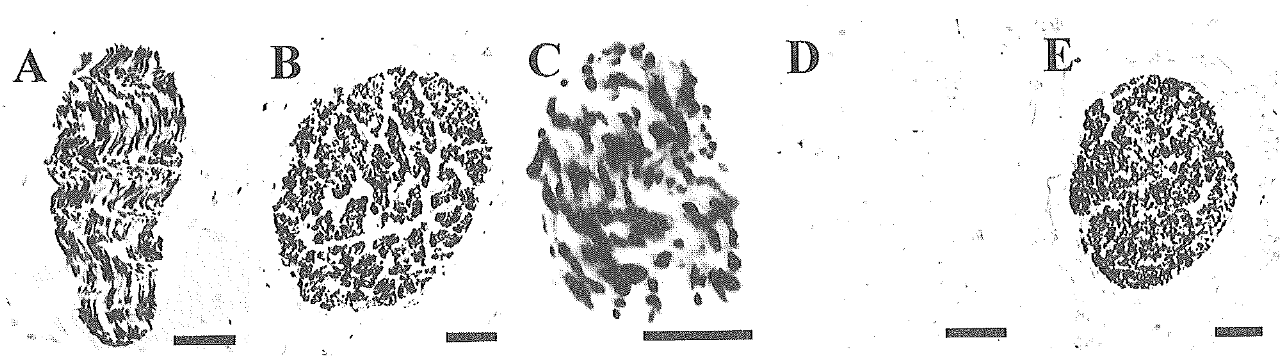

FIG. 2. Tyrosine hydroxylase (TH) immunostaining of the epicardium in the patients with PARK2 (**A–C**), the patient with PD (**D**), and the control subject (**E**). TH-immunoreactive nerve fibers are well preserved in the epicardium from the patient with PARK2 (A–C) and control subject (E), whereas those from the patient with PD (D) are absent. Scale bar = 20 μm.

Acknowledgments: This study was supported by the Japan Foundation for Neuroscience and Mental Health (Tama Nakagawa Foundation). We thank Dr. M. Takahashi for his helpful suggestion and Ms. Nakamura for her technical assistance.

REFERENCES

1. Kitada T, Asakawa S, Hattori N, et al. Mutations in the parkin gene cause autosomal recessive juvenile Parkinsonism. Nature 1998; 392:605–608.
2. Matsumine H, Saito M, Shimoda-Matsubayashi S, et al. Localization of a gene for an autosomal recessive form of juvenile Parkinsonism to chromosome 6q25.2-27. Am J Hum Genet 1997;60: 588–596.
3. Ishikawa A, Tsuji S. Clinical analysis of 17 patients in 12 Japanese families with autosomal-recessive type juvenile parkinsonism. Neurology 1996;47:160–166.
4. Takahashi H, Ohama E, Suzuki S, et al. Familial juvenile Parkinsonism: clinical and pathological study in a family. Neurology 1994;44:437–441.
5. Mori H, Kondo T, Yokochi M, et al. Pathological and biochemical studies of juvenile parkinsonism linked to chromosome 6p. Neurology 1998;51:890–892.
6. Hayashi S, Wakabayashi K, Ishikawa A, et al. An autopsy case of autosomal-recessive juvenile Parkinsonism with a homozygous exon 4 deletion in the *parkin* gene. Mov Disord 2000;15:884–888.
7. Tassin L, Durr A, de Broucker T, et al. Chromosomal 6-linked autosomal recessive early-onset parkinsonism: linkage in European and Algerian families, extension of the clinical spectrum, and evidence of a small homozygous deletion in one family—the French Parkinson's Disease Genetics Study Group, and the European Consortium on Genetic Susceptibility in Parkinson's Disease. Am J Hum Genet 1998;63:88–94.
8. Klein C, Plamstaller PP, Kis B, et al. Parkin deletion in a family with adult-onset, tremor-dominant Parkinsonism: expanding the phenotype. Ann Neurol 2000;48:65–71.
9. Yoshita M. Differentiation of idiopathic Parkinson's disease from striatonigral degeneration and progressive supranuclear palsy using iodine-123 meta-iodobenzylguanidine myocardial scintigraphy. J Neurol Sci 1998;155:60–67.
10. Orimo S, Ozawa E, Nakade S, Sugimoto T, Mizusawa H. ^{123}I-metaiodobenzylguanidine myocardial scintigraphy in Parkinson's disease. J Neurol Neurosurg Psychiatry 1999;67:189–194.
11. Braune S, Reinhardt M, Schnitzer R, Riedel A, Lücking CH. Cardiac uptake of [^{123}I] MIBG separates Parkinson's disease from multiple system atrophy. Neurology 1999;53:1020–1025.
12. Taki J, Nakajima K, Hwang E-H, et al. Peripheral sympathetic dysfunction in patients with Parkinson's disease without autonomic failure is heart selective and disease specific. Eur J Nucl Med 2000;27:566–573.
13. Orimo S, Ozawa E, Nakade S, et al. [^{123}I] MIBG myocardial scintigraphy differentiates corticobasal degeneration from Parkinson's disease. Intern Med 2003;42:127–128.
14. Goldstein DS, Holmes C, Li S-T, Bruce S, Metman LV, Cannon RO III. Cardiac sympathetic denervation in Parkinson disease. Ann Intern Med 2000;133:338–347.
15. Orimo S, Oka T, Miura H, et al. Sympathetic cardiac denervation in Parkinson's disease and pure autonomic failure but not in multiple system atrophy. J Neurol Neurosurg Psychiatry 2002;73: 776–777.
16. Amino T, Orimo S, Itoh Y, Takahashi A, Uchihara T, Mizusawa H. Profound cardiac sympathetic denervation occurs in Parkinson disease. Brain Pathol 2005;15:29–34.
17. Kitami T, Nomoto T, Nagao T, et al. ^{123}I-MIBG myocardial scintigraphy in juvenile Parkinsonism. Mov Disord 1998; 13(Suppl. 2):247.
18. Suzuki M, Hattori N, Orimo S, et al. Preserved myocardial ^{123}I-metaiodo-benzylguanidine uptake in autosomal recessive juvenile Parkinsonism: first case report. Mov Disord 2005;20:634–636.
19. Kawano H, Okada R, Yano K. Histological study on the distribution of autonomic nerves in the human heart. Heart Vessels 2003; 18:32–39.
20. Singleton A, Gwinn-Hardy K, Sharabi Y, et al. Association between cardiac denervation and Parkinsonism caused by α-synuclein gene triplication. Brain 2004;127:768–772.
21. Mitani I, Sumita S, Takahashi N, Ochiai H, Ishii M. ^{123}I-MIBG myocardial imaging in hypertensive patients: abnormality progresses with left ventricular hypertrophy. Ann Nucl Med 1996; 10:315–321.

Hum Genet (2005) 117: 520–527
DOI 10.1007/s00439-005-1342-8

ORIGINAL INVESTIGATION

Masayuki Ide · Kazuo Yamada · Tomoko Toyota
Yoshimi Iwayama · Yuichi Ishitsuka · Yoshio Minabe
Kazuhiko Nakamura · Nobutaka Hattori
Takashi Asada · Yoshikuni Mizuno · Norio Mori
Takeo Yoshikawa

Genetic association analyses of *PHOX2B* and *ASCL1* in neuropsychiatric disorders: evidence for association of *ASCL1* with Parkinson's disease

Received: 15 March 2005 / Accepted: 2 May 2005 / Published online: 14 July 2005

Abstract We previously identified frequent deletion/insertion polymorphisms in the 20-alanine homopolymer stretch of *PHOX2B* (*PMX2B*), the gene for a transcription factor that plays important roles in the development of oculomotor nerves and catecholaminergic neurons and regulates the expression of both tyrosine hydroxylase and dopamine β-hydroxylase genes. An association was detected between gene polymorphisms and overall schizophrenia, and more specifically, schizophrenia with ocular misalignment. These prior results implied the existence of other schizophrenia susceptibility genes that interact with *PHOX2B* to increase risk of the combined phenotype. *ASCL1* was considered as a candidate interacting partner of *PHOX2B*, as ASCL1 is a transcription factor that co-regulates catecholamine-synthesizing enzymes with PHOX2B. The genetic contributions of *PHOX2B* and *ASCL1* were examined separately, along with epistatic interactions with broader candidate phenotypes. These phenotypes included not only schizophrenia, but also bipolar affective disorder and Parkinson's disease (PD), each of which involve catecholaminergic function. The current case-control analyses detected nominal associations between polyglutamine length variations in *ASCL1* and PD ($P = 0.018$), but supported neither the previously observed weak association between *PHOX2B* and general schizophrenia, nor other gene-disease correlations. Logistic regression analysis revealed the effect of *ASCL1* dominant × *PHOX2B* additive ($P = 0.008$) as an epistatic gene–gene interaction increasing risk of PD. ASCL1 controls development of the locus coeruleus (LC), and accumulating evidence suggests that the LC confers protective effects against the dopaminergic neurodegeneration inherent in PD. The present genetic data may thus suggest that polyglutamine length polymorphisms in *ASCL1* could influence predispositions to PD through the fine-tuning of LC integrity.

M. Ide and K. Yamada contributed equally to this work

M. Ide · K. Yamada · T. Toyota · Y. Iwayama · Y. Ishitsuka
T. Yoshikawa (✉)
Laboratory for Molecular Psychiatry,
RIKEN Brain Science Institute, 2-1 Hirosawa,
Wako-city, Saitama 351-0198, Japan
E-mail: takeo@brain.riken.go.jp
Tel.: +81-48-4675968
Fax: +81-48-4677462

Y. Minabe · K. Nakamura · N. Mori
Department of Psychiatry and Neurology,
Hamamatsu University School of Medicine,
Hamamatsu 431-3192, Japan

N. Hattori · Y. Mizuno
Department of Neurology,
Juntendo University School of Medicine,
Tokyo 113-8421, Japan

T. Asada
Department of Psychiatry,
University of Tsukuba School of Medicine, Ibaraki 305-8576,
Japan

Introduction

Paired-like homeobox 2b (PHOX2B, also known as PMX2B or NBPhox) is a homeodomain transcription factor, and is known to determine noradrenergic phenotype (Pattyn et al. 2000) and play a role in the development of cranial motor nerves, including the oculomotor (nIII) and trochlear (nIV) nerves (Pattyn et al. 1997) controlling ocular alignment and movement. As a transcription factor, PHOX2B regulates the expression of tyrosine hydroxylase (TH) and dopamine β-hydroxylase (DBH) genes. TH catalyzes the conversion of L-tyrosine to L-dihydroxyphenylalanine (L-DOPA), a precursor of dopamine, and DBH catalyzes the conversion of dopamine to noradrenaline. The protein structure of PHOX2B is characterized by two

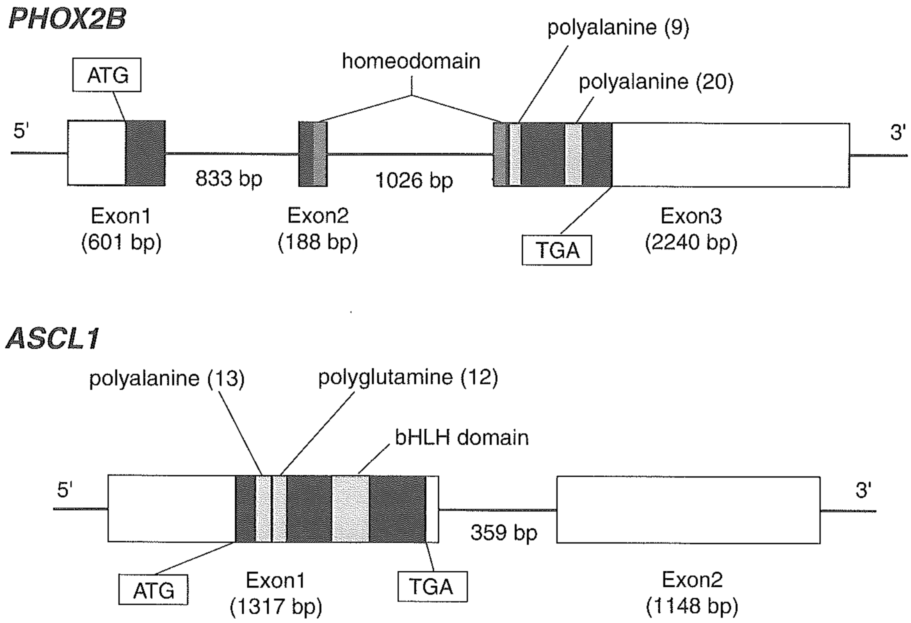

Fig. 1 Schematic representation of the *PHOX2B* (NM_003924) (*above*) and *ASCL1* (NM_004316) genes (*below*). Exons are *boxed*, and initiation and stop codons and protein domains are indicated

homopolymeric stretches of alanine residues: one consisting of nine alanines located downstream of the homeodomain; the other comprising 20 alanines (Ala20) on the C-terminal side (Fig. 1). Our prior genomic screening of *PHOX2B* identified frequent length variations in the Ala20 stretch in the general population, representing an unusual phenomenon compared with other polyalanine-containing transcription factors (Toyota et al. 2004). Variations included −3Ala, −5Ala, −7Ala, −13Ala and +2Ala. These alterations in alanine length resulted in decreased transcriptional ability of the protein and represented the only functional polymorphisms found in the gene. In accordance with the known function of PHOX2B and the functional consequences of these variations, associations between the polymorphisms and general schizophrenia were detected, particularly for schizophrenia manifesting with strabismus (ocular misalignment) (Toyota et al. 2004). That study also raised a possibility of interactions between *PHOX2B* and other schizophrenia-precipitating factors (genes) for increased risk of the combined phenotype (Toyota et al. 2004).

Human achaete-scute homologue 1 (HASH1; ASCL1 in HUGO nomenclature), a human orthologue of mouse Mash1, is a basic helix–loop–helix (bHLH) transcription factor that is known to co-regulate differentiation of the autonomic system along with PHOX2B (Pattyn et al. 2000). Cross-regulation by the *Phox2* and *Mash1* genes, and the importance of the HASH1-PHOX pathway in the development of neurons in the noradrenergic lineage have been demonstrated in both mice (Pattyn et al. 1999, 2000), and a human disease mechanism (De Pontual et al. 2003). We therefore speculated that *PHOX2B* and *ASCL1* may affect predispositions to broad catecholamine-related diseases both separately and in combination. The present study examined genetic associations between *PHOX2B* and *ASCL1* and schizophrenia, bipolar disorder and Parkinson's disease (PD).

Materials and methods

Study subjects

Subjects included 715 schizophrenic patients (394 men, mean age 48.3 ± 12.3 years; 321 women, mean age 50.7 ± 13.3 years), 249 bipolar disorder patients (118 men, mean age 52.6 ± 13.2 years; 131 women, mean age 55.8 ± 12.9 years), 100 PD patients (32 men, mean age 67.3 ± 7.8 years; 68 women, mean age 67.8 ± 7.0 years) and 801 healthy controls (369 men, mean age 40.9 ± 11.4 years; 432 women, mean age 41.3 ± 13.7 years). Compared with the prior study (Toyota et al. 2004), the number of schizophrenia patients was increased by 369 and the number of controls was increased by 260, but these newly added subjects were not screened for strabismus. All subjects were recruited from a geographic area located in central Japan. Diagnosis of schizophrenia and bipolar disorder was based on the *Diagnostic and statistical manual of mental disorders* (American Psychiatric Association 1994). PD was diagnosed according to the standardized criteria. All PD patients underwent brain computed tomography examination to exclude organic abnormalities. Control subjects were recruited from hospital staff and company employees who were documented as free of psychoses or any kind of neurodegenerative disorder. None of the current subjects displayed mental retardation or congenital central hypoventilation syndrome (De Pontual et al. 2003). This study was approved by the Ethics Committees of RIKEN, Hamamatsu University and Juntendo University, and all subjects provided written informed consent to participate.

Mutation screening of *ASCL1*

ASCL1 is located on human chromosome 12q22-q23 (Renault et al. 1995) and comprises two exons, with the first exon including both the initiation and stop codons (Fig. 1). The protein-coding region contains a polyalanine stretch comprising 13 alanines, and a polyglutamine tract of 12 glutamine residues (Gln12), in addition to the bHLH. The two exons and their flanking genomic stretches were screened using polymerase chain reaction (PCR) amplification and subsequent direct sequencing of genomic DNA from 24 randomly chosen patients. Sequencing was performed using a DYEnamic ET terminator cycle sequencing kit (Amersham, Piscataway, N.J., USA). Information on primer sequences and PCR conditions employed in this study is available on request. Screening detected the insertion of three CAG repeats (coding glutamine) into the polyglutamine stretch. This was the only non-synonymous polymorphism identified, and we therefore focused on this Gln12 length polymorphism in subsequent analyses.

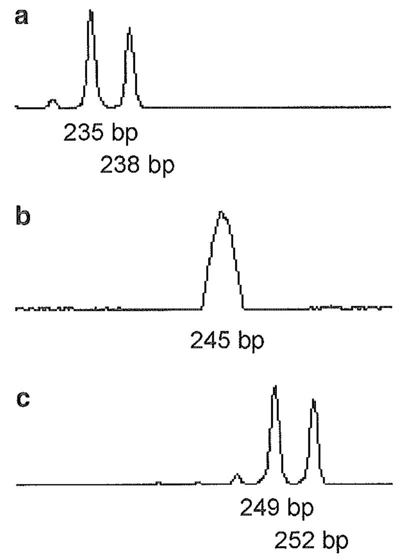

Fig. 2a–c GeneScan migration patterns of *ASCL1* Gln12 length polymorphisms. DNA fragments with Gln12 or Gln13 genotypes were run after PCR under varying concentrations of c^7 dGTP. Exact sizes of the Gln12 and Gln13 alleles were 249 and 252 bp, respectively. **a** The c^7 dGTP was not added to the PCR mixture. Note that displayed allele sizes were 14 bp shorter than actual sizes. **b** Addition of c^7 dGTP to 25% resulted in fusion of the two peaks. **c** When all dGTP in the PCR reaction mixture was replaced with c^7dGTP, peaks appeared at expected sizes with good separation of the two adjacent alleles

Genotyping

Genotyping of Ala20 length variations in the *PHOX2B* was performed according to the methods described elsewhere (Toyota et al. 2004). To genotype Gln12 polyglutamine length variations in *ASCL1*, template DNA was amplified using fluorescently labeled forward (5′-AGCTCTGCCAAGATGGAGAG; 3′ end at nt c.26) and reverse (5′- gtttcttTTGCTTGGGCGCTGACTTGT; 3′ end at nt c.236) primers. The *underlined* tail sequence was added because Taq DNA polymerase catalyzes the non-templated addition of adenosine to the 3′ end of PCR products to varying degrees. This phenomenon is primer-specific and represents a potential source of genotyping error. Placing the gtttctt sequence at the 5′ end of reverse primers produces nearly 100% adenylation of the 3′ end of the forward strand, facilitating accurate genotyping (Brownstein et al. 1996; I-tokawa et al. 2003). PCR products were run on an ABI 3700 genetic analyzer (Applied Biosystems, Foster City, Calif., USA), and the resulting data were analyzed using GeneScan software (Applied Biosystems). Genotypes were confirmed by subcloning the amplicons into a TA vector (Invitrogen, Carlsbad, Calif., USA) and sequencing. Primers were designed to produce a 249-bp DNA fragment for the wild-type allele (Gln12), but GeneScan analysis yielded a band approximately 14 bp shorter than expected (Fig. 2a), with occasional inconsistent genotype results compared with those obtained by subcloning, which could not be resolved by applying the constant 14-bp difference to GeneScan results. This phenomenon was attributed to the secondary DNA structure generated by abundant GCs in the PCR products (Toyota et al. 2004). When 7-deaza-2′-deoxyguanosine triphosphate (c^7 dGTP) was added to the PCR reaction mixture (c^7 dGTP:dGTP = 1:3) to breakdown hydrogen bonds in the GC-rich templates, GeneScan peaks were broadened and two adjacent peaks merged (Fig. 2b). We replaced all dGTP in the PCR reaction mixture with c^7 dGTP, and obtained sharp and correctly sized bands, enabling accurate genotyping (Fig. 2c).

Statistical analysis

Associations of either *PHOX2B* or *ASCL1* polymorphisms with each neuropsychiatric disorder were evaluated using the Monte–Carlo method implemented in the CLUMP program (T1–T4 modes; number of simulations set to 10,000; random number seed, 100) (Sham and Curtis 1995) or Fisher's exact test when appropriate. Rare alleles or genotypes showing frequencies of < 1% in both comparison groups were removed from the analysis. Hardy–Weinberg equilibrium was evaluated using Arlequin software (http://lgb.unige.ch/arlequin/) (Schneider and Excofier 2000). Logistic regression analysis in the SPSS Regression Models software (SPSS Japan, Tokyo, Japan) was performed to test the joint effects of the two genes. Letting P represent the probability of an individual being a case rather than a control, we modeled P as

$$\log \mathrm{it}(P) = \beta_0 + \sum_{i=1}^{4} \beta_i x_i + \sum_{i=1}^{2} \sum_{j=3}^{4} \beta_{ij} x_i x_j$$

where x_1, x_2, x_3 and x_4 represent covariants depending on the genotypes of the individual, β_0 is the intercept, and β_i and β_{ij} are coefficients to be estimated. When applied to the formula, genotypes were dichotomized into two groups: wild-type (w); and mutant (m). Following the approach of Cordell and Clayton (2002) for the possible genotypes of w/w, m/w and m/m, we coded -1, 0 and 1, respectively, to represent the additive effects of allele m and -0.5, 0.5, -0.5, respectively, to represent the dominant effect of allele m over allele w.

Results

Table 1 shows the results of association analyses between *PHOX2B* Ala20 length polymorphisms and the three disease categories. We detected six different genotypes, and distributions of genotypes in each group were all in Hardy–Weinberg equilibrium. None of the modes T1–T4 on CLUMP analysis displayed significant associations for any disease groups. The number of different alleles observed in this study was the same as in our previous study (Toyota et al. 2004), although much larger cohorts were examined here. Again, no allelic associations were detected for any of the three neuropsychiatric disorders.

Tables 2 and 3 show the results of genotypic and allelic analyses of *ASCL1* Gln12 stretch polymorphisms, respectively. Analysis of the 1,866 subjects yielded 13 different length variations in the Gln12 homopolyer repeat region of *ASCL1*. These polymorphisms were not genotypically associated with schizophrenia or bipolar disorder, but displayed associations with PD ($P < 0.05$ in T2, T3 and T4) (Table 2). Allelic analysis demonstrated that the allele containing 12 glutamine repeats, the most common of these alleles, was more frequent in PD than in the control group (2×2 Fisher's exact test, two-sided, $P = 0.015$; odds ratio = 1.68, 95% CI = 1.10–2.54), while the allele containing 15 glutamine repeats, as the second most common allele, exhibited an opposite distribution pattern ($P = 0.011$; odds ratio = 0.57, 95% CI = 0.36–0.89) (Table 3). These results suggest that the *ASCL1* allele harboring 15 glutamine repeats may play a protective role against PD manifestation.

Logistic regression analysis was then performed to test the joint effect of the two genes on PD. The Ala20 allele of *PHOX2B* and the Gln12 allele of *ASCL1* were classified as w, with the remaining alleles as m. As a result, only the effect of *ASCL1* dominant × *PHOX2B* additive was found to be significant ($P = 0.008$), among the effects of all possible interaction modes (Table 4).

Discussion

PHOX2B/*ASCL1* and psychiatric disorders

We have previously reported genotypic associations between Ala20 polymorphisms in *PHOX2B* and overall

Table 1 Genotypic and allelic distributions of the *PHOX2B* Ala20 repeat polymorphism

	Schizophrenia ($n = 715$)	Bipolar disorder ($n = 249$)	Parkinson's disease ($n = 100$)	Controls ($n = 802$)
Genotype[a]	Genotype counts (% frequency)			
15/15	0 (0)	0 (0)	1 (1.0)	3 (0.4)
20/7	1 (0.2)	0 (0)	0 (0)	0 (0)
20/13	6 (0.9)	2 (1.2)	0 (0)	7 (0.9)
20/15	57 (8.8)	14 (8.4)	9 (9.3)	59 (7.4)
20/20	579 (89.8)	151 (90.4)	87 (89.7)	727 (91.2)
20/22	2 (0.3)	0 (0)	0 (0)	1 (0.1)
P[b,c]				
T1	0.35	0.81	0.50	
T2	0.50	0.76	0.71	
T3	0.54	0.83	0.60	
T4	0.46	0.89	0.79	
Allele[a]	Allele counts (% frequency)			
7	1 (0.1)	0 (0)	0 (0)	0 (0)
13	6 (0.5)	2 (0.6)	0 (0)	7 (0.4)
15	57 (4.4)	14 (4.2)	11 (5.7)	65 (4.1)
20	1224 (94.9)	318 (95.2)	183 (94.3)	1521 (95.4)
22	2 (0.2)	0 (0)	0 (0)	1 (0.1)
P[b,d]	0.64	0.88	0.34	

[a]Number of alanine repeats
[b]Minor genotypes and alleles with frequencies (< 1% in both comparison groups were omitted from analyses
[c]Calculated using the Monte Carlo method
[d]Calculated using Fisher's exact test

Table 2 Genotypic distribution of the *ASCL1* Gln12 repeat polymorphism

	Schizophrenia ($n=715$)	Bipolar disorder ($n=249$)	Parkinson's disease ($n=100$)	Controls ($n=802$)
Genotype[a]	Genotype counts (% frequency)			
6/12	1 (0.1)	0 (0)	0 (0)	0 (0)
6/15	1 (0.1)	0 (0)	0 (0)	0 (0)
7/12	0 (0)	0 (0)	0 (0)	1 (0.1)
8/12	0 (0)	0 (0)	0 (0)	1 (0.1)
9/12	1 (0.1)	0 (0)	0 (0)	2 (0.3)
9/15	1 (0.1)	0 (0)	0 (0)	0 (0)
11/12	1 (0.1)	0 (0)	0 (0)	1 (0.1)
12/12	429 (61.5)	144 (60.0)	74 (75.5)	481 (61.0)
12/13	21 (3.0)	8 (3.3)	3 (3.1)	21 (2.7)
12/14	2 (0.3)	0 (0)	1 (1.0)	1 (0.1)
12/15	186 (26.6)	66 (27.5)	16 (16.3)	232 (29.4)
12/16	6 (0.9)	4 (1.7)	0 (0)	8 (1.0)
12/17	2 (0.3)	0 (0)	0 (0)	1 (0.1)
12/18	0 (0)	0 (0)	0 (0)	1 (0.1)
12/19	1 (0.1)	0 (0)	0 (0)	1 (0.1)
13/13	1 (0.1)	0 (0)	0 (0)	0 (0)
13/15	9 (1.3)	3 (1.3)	1 (1.0)	3 (0.4)
14/15	1 (0.1)	0 (0)	0 (0)	0 (0)
15/15	34 (4.9)	14 (5.8)	3 (3.1)	31 (3.9)
15/16	1 (0.1)	0 (0)	0 (0)	3 (0.4)
15/17	0 (0)	1 (0.4)	0 (0)	0 (0)
$P^{b,c}$				
T1	0.41	0.50	0.052	
T2	0.28	0.33	*0.016*	
T3	0.25	0.61	*0.010*	
T4	0.33	0.39	*0.046*	

[a] Number of glutamine repeats
[b] Minor genotypes and alleles with frequencies < 1% in both comparison groups were omitted from analyses
[c] Calculated using the Monte Carlo method

schizophrenia ($P=0.012$), with a more prominent association for schizophrenia with strabismus ($P=0.004$) (Toyota et al. 2004). However, the present study did not detect this association in a larger case-control panel with a 2.2-fold increase in the schizophrenia population and a 1.6-fold increase in control samples. This discrepancy may be partly due to the fact that prior control samples had undergone ocular examinations, and only those subjects who did not suffer from strabismus were chosen, while the present study used control samples with-

Table 3 Allelic distribution of the *ASCL1* Gln12 repeat polymorphism

	Schizophrenia ($n=715$)	Bipolar disorder ($n=249$)	Parkinson's disease ($n=100$)	Controls ($n=802$)
Allele[a]	Allele counts (% frequency)			
6	2 (0.1)	0 (0)	0 (0)	0 (0)
7	0 (0)	0 (0)	0 (0)	1 (0.1)
8	0 (0)	0 (0)	0 (0)	1 (0.1)
9	2 (0.1)	0 (0)	0 (0)	2 (0.1)
11	1 (0.1)	0 (0)	0 (0)	1 (0.1)
12	1079 (77.3)	366 (76.3)	168 (85.7)	1232 (78.2)
13	32 (2.3)	11 (2.3)	4 (2.0)	24 (1.5)
14	3 (0.2)	0 (0)	1 (0.5)	1 (0.1)
15	267 (19.1)	98 (20.4)	23 (11.7)	300 (19.0)
16	7 (0.5)	4 (0.8)	0 (0)	11 (0.7)
17	2 (0.1)	1 (0.2)	0 (0)	1 (0.1)
18	0 (0)	0 (0)	0 (0)	1 (0.1)
19	1 (0.1)	0 (0)	0 (0)	1 (0.1)
$P^{b,c}$				
T1	0.30	0.40	*0.036*	
T2	0.29	0.40	*0.022*	
T3	0.27	0.51	*0.018*	
T4	0.27	0.51	*0.026*	

[a]Number of glutamine repeats
[b]Minor genotypes and alleles with frequencies < 1% in both comparison groups were omitted from analyses
[c]Calculated using the Monte Carlo method

Table 4 Logistic regression analysis of effects of *PHOX2B* and *ASCL1* genes on Parkinson's disease

Variable	β[a]	SE[b]	Wald[c]	df[d]	*P*	Exp (β)[e]	95% CI[f]
ASCL1 dominant by *PHOX2B* additive	0.71	±0.27	7.0	1	0.008	2.0	1.2–3.4

[a]Logistic regression coefficient in the model
[b]Standard error of the coefficient
[c]Wald statistic to test significance of the coefficient
[d]Degrees of freedom for the Wald chi-square test
[e]Exponentiation of the β coefficient (odds ratio)
[f]95% confidence interval of exponentiation (β)

out determining the presence of ocular misalignment. The newly added schizophrenic samples in this study were also not screened for ocular misalignment. While the genetic contributions of *PHOX2B* Ala20 variations to general schizophrenia are more likely to be very weak or even negligible, even by considering genetic interactions with *ASCL1* (data not shown), these contributions may be evident only in a subset of schizophrenia (i.e., schizophrenia with strabismus). As might be expected according to this hypothesis, no association was apparent between *PHOX2B* and schizophrenia without strabismus ($P=0.076$) in our previous study (Toyota et al. 2004). We also tested here *ASCL1* as a singleton or *PHOX2B-ASCL1* epigenetic interaction (data not shown) for altered risk of another major psychosis, bipolar disorder, but no significant signals were detected. As a whole, the current results do not support these genetic mechanisms in the manifestation of functional psychoses.

PHOX2B/*ASCL1* and Parkinson's disease

PD is a common neurodegenerative disorder, characterized clinically by resting tremor, rigidity and bradykinesia. Neuropathological studies have revealed degeneration of the dopamine-producing substantia nigra and various other regions, including the basal ganglia, brainstem, autonomic nervous system and cerebral cortex (Dekker et al. 2003). Clinically defined PD represents an etiologically heterogeneous group of conditions encompassing a small population of individuals with Mendelian-type inheritance and a larger population of apparently sporadic cases (Hattori et al. 2003). Accumulating evidence has suggested that genetic predispositions exist even for sporadic PD (Marder et al. 1996). Dopamine deficiency is a primary pathomechanism in PD, and genes involved in dopamine neurotransmission, such as those for dopamine transporter, dopamine receptors, tyrosine hydroxylase, catechol-it O-methyltransferase and monoamine oxidase, have been examined in population-based association studies over the past decade. However, few of these genes have been definitively established as conferring susceptibility to sporadic PD (reviewed in Warner and Schapira 2003).

Perturbation of *PHOX2B* and *ASCL1* function has the potential to disturb catecholaminergic neurons, as these genes control the expression of the *TH* and *DBH* genes, which encode enzymes for the biosynthesis of dopamine (TH) and noradrenalin (TH and DBH) biosynthesis. Ludecke et al. (1996) reported a female infant who manifested L-dopa responsive Parkinsonism and carried a Leu^{205}Pro mutation in exon 5 of the *TH* gene, reducing the catalytic ability of TH. The current study identified a positive association between PD and *ASCL1* polymorphisms. However, whether these *ASCL1* variants result in a predisposition to PD through direct effects on dopamine neurons remains unclear, as *ASCL1* expression in the human substantia nigra has not yet been confirmed. In contrast, expression of *ASCL1* in developing noradrenergic neurons in the human brainstem (locus coeruleus: LC) has been reported (De Pontual et al. 2003). The LC is known to play an important role in the pathophysiology of PD (reviewed in Gesi et al. 2000). Zarow et al. (2003) found more severe neuronal loss in the LC than in the substantia nigra in a postmortem examination of brains from PD patients. Mavridis et al. (1991) demonstrated that monkeys with LC lesions displayed impaired recovery from Parkinsonism induced using 1-methyl-4-phenyl-1,2,3,6-tetrahydropyridine (MPTP). Other studies have also shown that animals with LC lesions exhibit marked dopamine loss on administration of MPTP or methamphetamine (Bing et al. 1994; Fornai et al. 1997). These data suggest a protective role of the LC against the development of PD. Indeed, Srinivasan and Schmidt (2004) reported that the enhancement of noradrenergic transmission in the LC by β_2-adrenoceptor antagonists exerts a prophylactic effect against 6-hydroxydopamine-induced Parkinsonism. The present finding that the *ASCL1* allele containing 15 glutamines is less represented in PD than in controls might suggest that the 15-repeat allele could confer protective benefits compared to the most common 12-repeat allele, perhaps allowing the development of a well-functionalized LC that in turn helps to protect the substantia nigra from various insults.

Because of the presumed multigenic nature of complex traits, it would be desirable to analyze several polymorphisms jointly and investigate their effects and possible interactions on disease outcome (Ott 2001). One of the statistical methods that can be used to resolve this problem is logistic regression analysis. When applied to the current data, this analysis indicated that the dominant effect of *ASCL1* with the additive effect of *PHOX2B* was positive. The biological consequences resulting from the interaction between *ASCL1* and *PHOX2B* might thus offer useful insights into the pathogenesis of PD. Further studies elucidating the detailed mechanisms of this interaction are thus warranted.

Polyglutamine length variations in *ASCL1*

Polyglutamine expansion has been found in various neurodegenerative disorders, including Huntington's disease, spinocerebellar ataxia types 1, 2, 3 and 7, dentatorubral-pallido-luysian atrophy and spinobulbar muscular atrophy (Lipinski and Yuan 2004). The aggregation or accumulation of proteins with expanded polyglutamine sequences is considered to represent a critical contribution to neurodegeneration in these diseases. Generally these aggregate-forming proteins display more than 30 glutamine repeats, while *ASCL1* displays repeats of less than 20 glutamines. None of the Gln12 length variations for *ASCL1* detected in this study are thus likely to exert deteriorative effects on neurons. However, the functional consequences evoked by variations of the polyglutamine stretch in *ASCL1* are yet to be examined.

In summary, we performed an association study for *PHOX2B* and *ASCL1*, genes that are functionally closely related and display imperative roles in the development of neurons in the noradrenergic (dopaminergic) lineage, in three major neuropsychiatric diseases. Significant contributions of *ASCL1* and *ASCL1-PHOX2B* interactions to PD were detected. These results require genetic replication studies in different populations and further biological investigations to clarify the precise mechanisms and effects.

Acknowledgements This work was supported by RIKEN BSI Funds, Research on Brain Science Funds from the Ministry of Health Labor and Welfare, CREST funds from the Japan Science and Technology Agency and grants from the MEXT of Japan. We wish to thank Ms Ohba for technical assistance and the members of the Research Resource Center at the RIKEN Brain Science Institute for genotyping services.

References

American Psychiatric Association (1994) Diagnostic and statistical manual of mental disorders, 4th edn. American Psychiatric Association, Washington, D.C.

Bing G, Zhang Y, Watanabe Y, McEwen BS, Stone EA (1994) Locus coeruleus lesions potentiate neurotoxic effects of MPTP in dopaminergic neurons of the substantia nigra. Brain Res 668:261–265

Brownstein MJ, Carpten JD, Smith JR (1996) Modulation of non-templated nucleotide addition by Taq DNA polymerase: primer modifications that facilitate genotyping Biotechniques 20:1004–1006, 1008–1010

Cordell HJ, Clayton DG (2002) A unified stepwise regression procedure for evaluating the relative effects of polymorphisms within a gene using case/control or family data: application to HLA in type 1 diabetes. Am J Hum Genet 70:124–141

De Pontual L, Nepote V, Attie-Bitach T, Al Halabiah H, Trang H, Elghouzzi V, Levacher B, Benihoud K, Auge J, Faure C, Laudier B, Vekemans M, Munnich A, Perricaudet M, Guillemot F, Gaultier C, Lyonnet S, Simonneau M, Amiel J (2003) Noradrenergic neuronal development is impaired by mutation of the proneural *HASH-1* gene in congenital central hypoventilation syndrome (Ondine's curse). Hum Mol Genet 12:3173–3180

Dekker MC, Bonifati V, Van Duijn CM (2003) Parkinson's disease: piecing together a genetic jigsaw. Brain 126:1722–1733

Fornai F, Alessandri MG, Torracca MT, Bassi L, Corsini GU (1997) Effects of noradrenergic lesions on MPTP/MPP+ kinetics and MPTP-induced nigrostriatal dopamine depletions. J Pharmacol Exp Ther 283:100–107

Gesi M, Soldani P, Giorgi FS, Santinami A, Bonaccorsi I, Fornai F (2000) The role of the locus coeruleus in the development of Parkinson's disease. Neurosci Biobehav Rev 24:655–668

Hattori N, Kobayashi H, Sasaki-Hatano Y, Sato K, Mizuno Y (2003) Familial Parkinson's disease: a hint to elucidate the mechanisms of nigral degeneration. J Neurol 250(Suppl 3):III2–10

Itokawa M, Yamada K, Yoshitsugu K, Toyota T, Suga T, Ohba H, Watanabe A, Hattori E, Shimizu H, Kumakura T, Ebihara M, Meerabux JMA, Toru M, Yoshikawa T (2003) A microsatellite repeat in the promoter of the NMDA receptor 2A subunit (*GRIN2A*) gene suppresses transcriptional activity and correlates with chronic outcome in schizophrenia. Pharmacogenetics 13:271–278

Lipinski MM, Yuan J (2004) Mechanisms of cell death in polyglutamine expansion diseases. Curr Opin Pharmacol 4:85–90

Ludecke B, Knappskog PM, Clayton PT, Surtees RA, Clelland JD, Heales SJ, Brand MP, Bartholome K, Flatmark T (1996) Recessively inherited L-DOPA-responsive Parkinsonism in infancy caused by a point mutation (L205P) in the tyrosine hydroxylase gene. Hum Mol Genet 5:1023–1028

Marder K, Tang MX, Mejia H, Alfaro B, Cote L, Louis E, Groves J, Mayeux R (1996) Risk of Parkinson's disease among first-degree relatives: a community-based study. Neurology 47:155–160

Mavridis M, Degryse AD, Lategan AJ, Marien MR, Colpaert FC (1991) Effects of locus coeruleus lesions on parkinsonian signs, striatal dopamine and substantia nigra cell loss after 1-methyl-4-phenyl-1,2,3,6-tetrahydropyridine in monkeys: a possible role for the locus coeruleus in the progression of Parkinson's disease. Neuroscience 41:507–523

Ott J (2001) Neural networks and disease association studies. Am J Hum Genet 105:60–61

Pattyn A, Morin X, Cremer H, Goridis C, Brunet JF (1997) Expression and interactions of the two closely related homeobox genes *Phox2a* and *Phox2b* during neurogenesis. Development 124:4065–4075

Pattyn A, Morin X, Cremer H, Goridis C, Brunet JF (1999) The homeobox gene *Phox2b* is essential for the development of autonomic neural crest derivatives. Nature 399:366–370

Pattyn A, Goridis C, Brunet JF (2000) Specification of the central noradrenergic phenotype by the homeobox gene *Phox2b*. Mol Cell Neurosci 15:235–243

Renault B, Lieman J, Ward D, Krauter K, Kucherlapati R (1995) Localization of the human achaete-scute homolog gene (*ASCL1*) distal to phenylalanine hydroxylase (*PAH*) and proximal to tumor rejection antigen (*TRA1*) on chromosome 12q22-q23. Genomics 30:81–83

Schneider RD, Excofier L (2000) Arlequin: a software for population genetics data analysis, 2 edn, version 2.000. Genetics and Biometry Laboratory, Department of Anthropology, University of Geneva

Sham PC, Curtis D (1995) Monte Carlo tests for associations between disease and alleles at highly polymorphic loci. Ann Hum Genet 59:97–105

Srinivasan J, Schmidt WJ (2004) Treatment with alpha2-adrenoceptor antagonist, 2-methoxy idazoxan, protects 6-hydroxy-dopamine-induced Parkinsonian symptoms in rats: neurochemical and behavioral evidence. Behav Brain Res 154:353–363

Sriuranpong V, Borges MW, Strock CL, Nakakura EK, Watkins DN, Blaumueller CM, Nelkin BD, Ball DW (2002) Notch signaling induces rapid degradation of achaete-scute homolog 1. Mol Cell Biol 22:3129–3139

Toyota T, Yoshitsugu K, Ebihara M, Yamada K, Ohba H, Fukasawa M, Minabe Y, Nakamura K, Sekine Y, Takei N, Suzuki K, Itokawa M, Meerabux JMA, Iwayama-Shigeno Y, Tomaru Y, Shimizu H, Hattori E, Mori N, Yoshikawa T (2004) Association between schizophrenia with ocular misalignment and polyalanine length variation in PMX2B. Hum Mol Genet 13:551–561

Warner TT, Schapira AH (2003) Genetic and environmental factors in the cause of Parkinson's disease. Ann Neurol 53 (Suppl 3):S16–S23

Zarow C, Lyness SA, Mortimer JA, Chui HC (2003) Neuronal loss is greater in the locus coeruleus than nucleus basalis and substantia nigra in Alzheimer and Parkinson diseases. Arch Neurol 60:337–341

FEBS Letters 580 (2006) 474–478

Dominant-negative effect of mutant valosin-containing protein in aggresome formation

Makiko-Iijima Kitami[a], Toshiaki Kitami[a], Masami Nagahama[c], Mitsuo Tagaya[c], Seiji Hori[d], Akira Kakizuka[d], Yoshikuni Mizuno[a,b], Nobutaka Hattori[a,b,*]

[a] *Department of Neurology, Juntendo University School of Medicine, 2-1-1 Hongo, Bunkyo, Tokyo 113-0033, Japan*
[b] *Research Institute for Diseases of Old Age, Juntendo University School of Medicine, Tokyo, Japan*
[c] *School of Life Science, Tokyo University of Pharmacy and Life Science, Hachioji, Tokyo, Japan*
[d] *Laboratories of Functional Biology, Kyoto University School of Biostudies, Kyoto, Japan*

Received 21 September 2005; revised 9 November 2005; accepted 13 December 2005

Available online 22 December 2005

Edited by Horst Feldmann

Abstract Lewy bodies (LBs) are the pathologic hallmark of Parkinson's disease. Recent studies revealed that LBs exhibit several morphologic and molecular similarities to aggresomes. Aggresomes are perinuclear aggregates representing intracellular deposits of misfolded proteins. Recently, valosin-containing protein (VCP) was one of the components of LBs, suggesting its involvement in LB formation. Here, we showed the localization of VCP in aggresomes induced by a proteasome inhibitor in cultured cells. Cells overexpressing mutant VCP (K524M: D2) showed reduced aggresome formation relative to those overexpressing wild-type and mutant (K251M: D1) VCPs. Our findings suggest that the D2 domain is involved in aggresome formation.

Keywords: Valosin-containing protein; Parkinson's disease; Lewy body; Aggresome

1. Introduction

Parkinson's disease (PD) is characterized histopathologically by the relatively selective loss of dopaminergic neurons in the substantia nigra and the presence of Lewy bodies (LBs) [1]. Recent studies suggest that LBs are related to aggresomes [2]. The latter are formed upon exhaustion of neuronal cell machinery responsible for the degradation of misfolded proteins [3]. Furthermore, aggresomes are formed at the microtubule (MT)-organizing center (MTOC) and are defined as pericentriolar membrane-free cytoplasmic inclusions that contain misfolded, ubiquitinated proteins ensheathed in a cage of the intermediate filament (IF) protein, vimentin [3,4].

Valosin-containing protein (VCP) is a 97-kDa protein and a member of type II ATPases associated with a variety of cellular activities (AAA), which are characterized by the presence of two conserved ATPase domains, also called AAA domains [5]. Recent studies revealed that VCP acts as a molecular chaperone in many apparently unrelated cellular activities [6]. Among these activities, VCP recognizes misfolded proteins such as polyglutamine [7]. Indeed, VCP is recognized in nuclear inclusion bodies of polyglutamine diseases [8]. Moreover, VCP is also recognized in LBs of PD [8,9].

Based on the above background, we postulated that VCP is involved in the formation of aggresomes. To test this, we examined the induction of VCP in aggresomes of cells treated with a proteasome inhibitor, MG132, and the role of VCP in aggresome formation.

2. Materials and methods

2.1. Plasmids and antibodies

We constructed pUHD10-3/VCP^{WT}-Myc, pCMV/FLAG-6c-VCP^{WT}, and pCMV/FLAG-6c-VCP$^{K251M/K524M}$ for this experiment. pUHD10-3/VCP^{WT}-Myc was digested and inserted into the *Xho*I site of the pcDNA3.1 vector (Invitrogen). pcDNA3.1/FLAG-VCP^{WT} was prepared by polymerase chain reaction (PCR) using appropriately designed primers with restriction site (*Bam*HI). The PCR product was inserted into the pcDNA3.1 vector. pcDNA3.1/FLAG-VCP^{K251M}, FLAG-VCP^{K524M} were prepared by using QuikChange Site-Directed Mutagenesis Kit (Stratagene). These point mutants lack two ATPases activity domains such as D1 and D2 [8]. pcDNA3.1/α-synuclein^{WT} and pcDNA3.1/FLAG-IκBα^{WT} were kind gifts from Drs. Suzuki and Chiba (The Tokyo Metropolitan Institute of Medical Science, Tokyo). We prepared FLAG-tagged α-synuclein to examine the interaction between VCP and α-synuclein.

The following antibodies were used in the present study; anti-VCP polyclonal antibody (Santa Cruz), anti-ubiquitin monoclonal antibody (Chemicon), anti-FLAG polyclonal antibody (Affiniti), anti-FLAG-HRP (Affiniti), anti-Myc monoclonal antibody (Santa Cruz), anti-vimentin monoclonal antibody (Sigma), anti-β actin monoclonal antibody (Sigma), anti-γ-tubulin monoclonal antibody (Sigma), and anti-Hsp70 antibody (BD Transduction Laboratories).

2.2. Cell culture and transfection

Kidney cell lines, HEK293 cells were grown in Dulbeccos modified Eagle's medium (DMEM) containing 10% fetal bovine serum (FBS), 100 U/ml penicillin and 100 μg/ml streptomycin. Confluent cells were transfected with 9 μg Myc-vector, VCP^{WT}-Myc, 5 μg FLAG-α-synuclein and 2 μg FLAG-IκBα. At 24 h after transfection, the cells were lysed with 500 μl lysis buffer (150 mM NaCl, 50 mM Tris–HCl [pH 7.5], 1.0% nonidet-P40, 10% glycerol, 1 M dithiothreitol) and protease inhibitor cocktail; Complete Mini. The lysate was then centrifuged at 17 000 × *g* for 15 min at 4 °C, and then 30 μl volume of the supernatant was used as the "lysate" for SDS–PAGE, while 450 μl volume of the supernatant was used for immunoprecipitation. For immunoprecipitation, 2 μg anti-Myc antibody was added to each 450 μl of the supernatant and the mixture was rotated for 3 h at 4 °C, then centrifuged at 17 000 × *g* for 15 min. The supernatants were mixed with 20 μl protein G-Sepharose (Amersham Biosciences), rotated for 3 h at 4 °C, then

*Corresponding author. Fax: +81 3 3813 7440/5800 0547.
E-mail address: nhattori@med.juntendo.ac.jp (N. Hattori).

0014-5793/$32.00
doi:10.1016/j.febslet.2005.12.044

centrifuged at 1800 × g for 5 min, washed three times and then mixed with 30 μl of the sample buffer. The samples were separated by SDS–PAGE (10–20% gradient gel) and transferred onto a PVDF membrane. Finally, detection was performed with anti-FLAG-HRP antibody (1:2000) and anti-Myc monoclonal antibody (1:2000).

2.3. Cell culture and immunological analysis

SH-SY5Y neuroblastoma cell and HEK 293 cells were grown in DMEM containing 10% FBS, 100 U/ml penicillin and 100 μg/ml streptomycin. Confluent cells were treated with 10 μM MG132 (Sigma), proteasome inhibitor and dimethyl sulfoxide (DMSO; Sigma) (for control) for 0, 4, or 8 h. The cells were lysed with lysis buffer (150 mM NaCl, 50 mM Tris–HCl [pH 7.5], 1.0% nonidet-P40, 10% glycerol and cocktail: Complete Mini; Roche). The lysate was then centrifuged at 17000 × g for 15 min at 4 °C. Next, the supernatant was used as the "crude". We considered the presence of aggregation in the pellet fraction and accordingly the pellet was solubilized with a mixture of 6 M urea, 50 mM Tris–HCl [pH 7.5], and 5 mM 2-mercaptoethanol, and sonicated. We then added the sample buffer to the sonicated sample as the "pellet". The whole lysates were prepared using the same method. The samples were separated by SDS–PAGE and transferred onto a PVDF membrane. Finally, detection was performed with VCP polyclonal and ubiquitin monoclonal antibodies.

2.4. Immunohistochemistry

After growing on 35-mm dishes (with glass coverslips), SH-SY5Y or HEK293 cells were treated with 10 μM MG132 or DMSO for 24 h. The cells were fixed in 4% paraformaldehyde in PBS for 30 min and permealized with Triton-X 100 for 20 min. Then, the cells were blocked overnight at 4 °C with 4% normal goat serum in PBS, incubated overnight with anti-VCP and anti-ubiquitin, anti-vimentin, anti-γ-tubulin, anti-Hsp70, and anti-FLAG antibodies in each case, washed with 0.01% Triton-X 100, and incubated for 30 min with Alexa 543 nm anti-mouse antibody and FITC 488 nm anti-rabbit antibody. The coverslips were washed and mounted on one vectashield. Fluorescence images were obtained using a fluorescence microscope.

2.5. Cell viability

HEK293 cells were grown under the same conditions. Confluent cells were transfected with 5 μg of FLAG-vector, FLAG-VCP^{WT}, FLAG-VCP^{K251M}, FLAG-VCP^{K524M}, or FLAG-VCP$^{K251M/K524M}$. The next day, the cells were transferred to 96-well dishes. After 1 h, the cells were treated with 10 μM MG132 or DMSO, and the cell viability was analyzed the next day. We used the MTT [3-(4,5-dimethylthiazol-2-yl)-2,5-diphenyltetrazolium bromide] reduction assay kit (Dojindo). We repeated the same experiments four times. To confirm the efficiencies of expression level, transfected cells were lysed with lysis buffer and centrifuged. We then added the sample buffer to the supernatant samples and applied them on the SDS–PAGE. In addition, we performed Western blotting with anti-FLAG, anti-VCP and anti-β-actin antibodies.

3. Results and discussion

Recent studies showed that cells treated with MG132 form aggregates that resemble LBs [10]. We first investigated whether VCP exists in such aggregates. As shown in Fig. 1, VCP was found in an aggregate formed under MG132. We also found that VCP levels were increased in the insoluble fraction, similar to polyubiquitinated proteins under MG132 condition, but not DMSO (Fig. 2). This finding indicates that these aggresomes were detergent insoluble and that VCP and ubiquitinated proteins were components of this fraction. Under this condition, the supernatant VCP fraction did not decrease at the same time, suggesting upregulation of VCP in the detergent-insoluble fraction. On the other hand, no increase in the whole VCP fraction was detected, suggesting that the amounts of supernatant fractions were larger than the insoluble fractions.

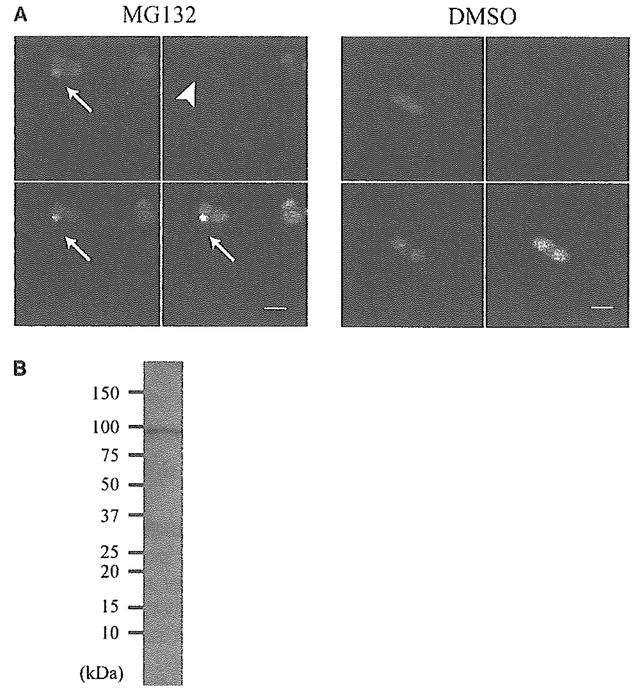

Fig. 1. Subcellular localization of endogenous VCP and ubiquitin in SH-SY5Y cells treated or untreated with a proteasome inhibitor. SH-SY5Y cells were treated with 10 μM MG132 (A) or DMSO (B) for 24 h. Cells were stained with anti-VCP and anti-ubiquitin antibodies. Nuclei were stained with DAPI (blue). FITC (green) and Alexa (red) correspond to VCP and ubiquitin, respectively. After treatment with MG132, both VCP and ubiquitin showed perinuclear accumulation and colocalization and appeared as clear protein aggregates (arrows). Nuclear torsion was observed (arrowhead). Scale bar = 20 μm.

In the next step, we investigated the localization of endogenous VCP in aggresomes. VCP formed a single large perinuclear aggresome-like structure and was co-localized with ubiquitin. Nuclear torsion was also noted (Fig. 1). Then we characterized the structure of these aggresomes to determine whether it is similar to that of typical aggresomes [3]. As shown in Fig. 3A, VCP-positive aggresomes were surrounded by vimentin in MG132-treated cells. Aggregates of misfolded proteins that escape degradation are targeted and accumulate in the MTOC. Subsequently, aggresomes are formed in the MTOC [3]. First, we showed that VCP-positive aggresomes co-localized with γ-tubulin, a marker of MTOC (Fig. 3B). Second, aggresomes are also abundant in chaperones such as Hsp70 [11]. We observed that Hsp70 co-localized with VCP in such aggresomes (Fig. 3C). Finally, we investigated the effect of inhibition of microtubule dynamics using an anti-mitotic agent, nocodazole, on the formation of these aggresomes. Co-incubation of cells with 10 μM nocodazole and MG132 resulted in inhibition of aggresome formation as evident in VCP and vimentin staining (Fig. 3D). These results indicate that the VCP-positive aggregates in SH-SY5Y cells are typical aggresomes.

We next examined the involvement of VCP in aggresome formation. We prepared FLAG-vector, FLAG-VCP^{WT}, FLAG-VCP^{K251M}, FLAG-VCP^{K524M}, and FLAG-VCP$^{K251M/K524M}$. The latter three vectors encode proteins lacking the function of two ATPase domains, D1 and D2, respectively. Considering the transfection efficiency, we used

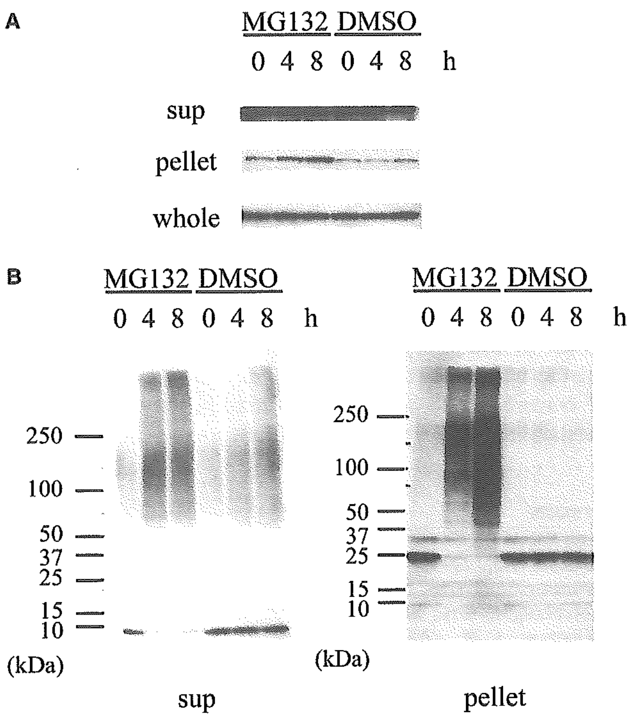

Fig. 2. Endogenous VCP moved to insoluble fraction similar to polyubiquitin under treatment with proteasome inhibitor. Cells were treated with 10 μM MG132 and DMSO for 0, 4 and 8 h. While VCP was identified in the supernatant fraction (A), it moved to the insoluble fraction (A) similar to polyubiquitin in MG132-treated cells (B).

HEK293 cells instead of SH-SY5Y cells. In this regard, the mechanisms of aggresome formation have been well studied in HEK293 cell lines [3]. The proportions of aggresomes-containing FLAG-VCP^{K524M}- and FLAG-VCP$^{K251M/K524M}$-transfected HEK293 cells were significantly lower than others (Fig. 4A). However, there was no significant difference in cell viability among FLAG-VCP^{K524M}-, FLAG-VCP$^{K251M/K524M}$-transfected HEK293 cells and cells transfected with other plasmids before treatment with MG132, as FLAG-VCP^{K524M} and FLAG-VCP$^{K251M/K524M}$ mutants tended to induce cell loss. In contrast, treatment with MG132 significantly influenced the viability of cells overexpressing FLAG-VCP^{K524M}, FLAG-VCP$^{K251M/K524M}$, and others. Considering the enhancement effects of MG132, we calculated the ratio of cell viability under DMSO and MG132, e.g., the ratio of FLAG-VCP^{WT}/FLAG-vector (under MG132) and FLAG-VCP^{WT}/FLAG-vector (under DMSO). There was no significant difference among the transfected cells. Thus, cell death of HEK293 cells with different expression vectors was similar under MG132 (Fig. 4B). Furthermore, the expression levels of exogenous FLAG-vectors were almost equal, suggesting that the transfection efficiencies of the vectors are similar. Indeed, the ratios of endogenous VCP to transfected FLAG-VCPs were almost 1:1 (Fig. 4C). These results suggest that the D2 domain of VCP is required for the formation of aggresomes rather than for cell death. Hirabayashi et al. [8] reported that cell viability was significantly reduced in mutant D2 VCP-transfected cells. In the previous report, the increased ratio of transfected mutant D2 VCP to wild-type VCP was inversely associated with cell viability. The discrepancy may be due to the different expression level of mutant VCP.

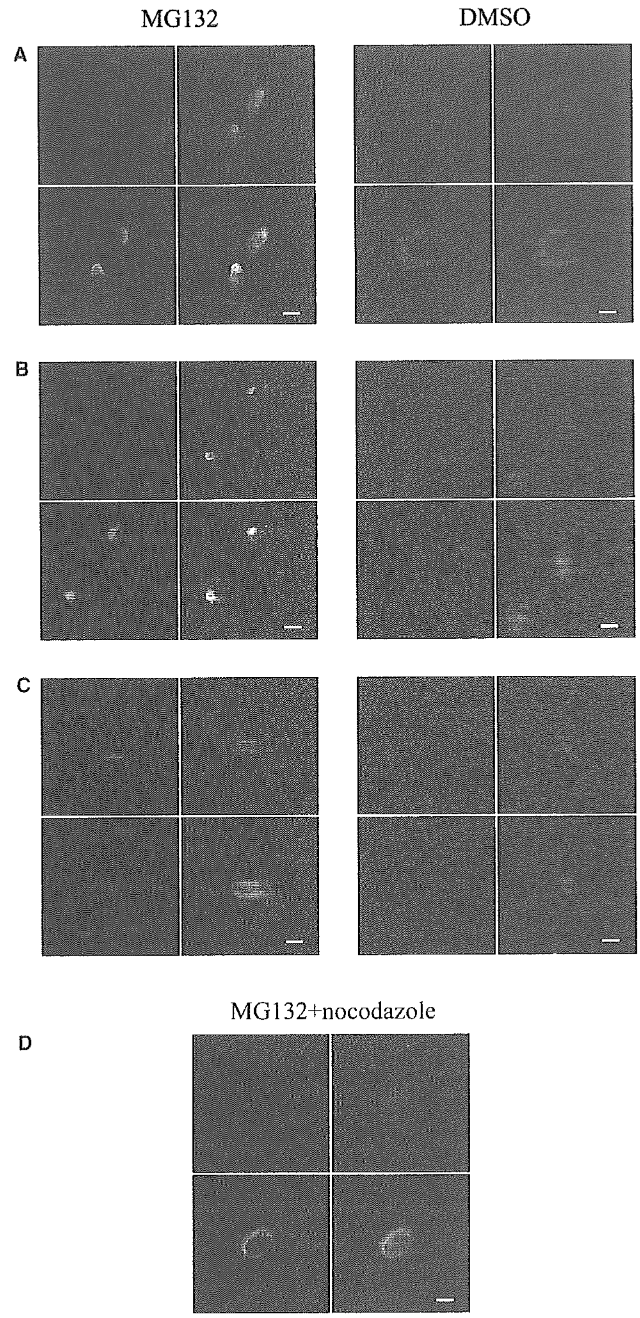

Fig. 3. VCP-positive aggregates are aggresomes. SH-SY5Y cells were treated with 10 μM MG132 or DMSO for 24 h, then stained with anti-VCP (A–D), anti-vimentin (A, D), anti-γ-tubulin (B) or anti-Hsp70 antibodies (C). Nuclei were stained with DAPI (blue). FITC (green) represents VCP and Alexa (red) represents vimentin (A, D), γ-tubulin (B) or Hsp70 (C). In MG132-treated cells, VCP-positive aggregates are surrounded by vimentin (A). Co-localization studies with anti-VCP and γ-tubulin antibodies showed VCP-positive aggresomes co-localized with γ-tubulin in MG132-treated cells (B). Hsp70 also co-localized with VCP-positive aggresomes (C). Inhibition of microtubule dynamics by antimitotic agent, nocodazole, was associated with inhibition of VCP and vimentin staining in MG132-treated cells (D; nocodazole and MG132). Scale bar = 20 μm.

As reported previously [8,9], VCP is localized in LBs of PD patients. Thus, it is possible that VCP interacts with α-synuclein within LBs. However, wild-type VCP did not interact with α-synuclein while IκBα as a positive control interacted with

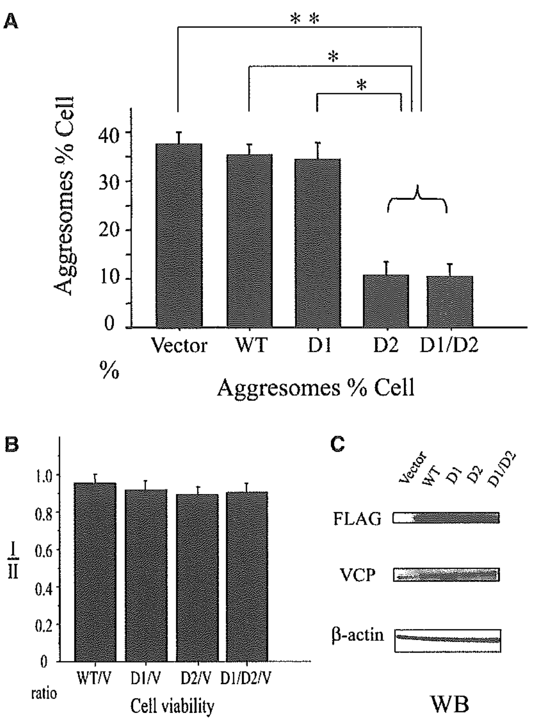

Fig. 4. Overexpression of VCPs affects aggresome formation. (A) HEK293 cells were transfected with FLAG-vector, FLAG-VCP^{WT}, FLAG-VCP^{K251M}, FLAG-VCP^{K524M}, or FLAG-VCP$^{K251M/K524M}$ vectors. The cells were then treated with MG132 after 24 h and harvested at 48 h after transfection. Anti-FLAG antibody and anti-vimentin antibody were used for detection of aggresome-containing transfected cells. Data are mean ± S.D. of the proportion of aggresome-containing cells. $^{*}P < 0.005$, $^{**}P < 0.01$, by Student's paired *t*-test. (B) Cell viability was analyzed using MTT assay. There was no significant difference among the ratios of each overexpression FLAG-VCP^{WT}, FLAG-VCP^{K251M}, FLAG-VCP^{K524M}, and FLAG-VCP$^{K251M/K524M}$ cells. (I = FLAG-VCP^{WT}, FLAG-VCP^{K251M}, FLAG-VCP^{K524M}, or FLAG-VCP$^{K251M/K524M}$/FLAG-vector [under MG132 treatment]), II = FLAG-VCP^{WT}, FLAG-VCP^{K251M}, FLAG-VCP^{K524M}, or FLAG-VCP$^{K251M/K524M}$/FLAG-vector [under DMSO treatment]. (C) Wild-type and mutant FLAG-VCPs and FLAG-vector were only expressed in HEK293 cells. Immunoblotting was performed with anti-FLAG, anti-VCP and anti-β-actin antibodies. The ratio of endogenous VCP to transfected FLAG-VCPs was 1:1.

VCP, as reported previously (data not shown) [12]. The results suggest that VCP and α-synuclein do not interact directly with each other.

VCP consists of two ATP binding sites: D1, which exhibits a heat-enhanced ATPase activity, and D2, which exhibits ATPase activity. D1 is responsible for the formation of stable hexamers while D2 has a major ATPase activity [6,13,14]. The ATPase activity of VCP is modulated by various environmental factors, similar to molecular chaperones. In the present study, fewer cells with aggresomes were noted among the cells transfected with D2 mutant VCP. In contrast, the proportion of aggresomes-containing cells was not significantly different between wild-type VCP- and mock-transfected cells, suggesting that endogenous VCP is involved in aggresome formation. Therefore, the D2 mutant VCP reduced the frequency of aggresomes as a dominant negative effect. On one hand, the lack of increment in wild-type VCP suggests that there is some rate-control process in aggresome formation. For example, dynein motor protein contributes to aggresome formation, and this step is thought to be a physically a rate-controlling step [3,15,16]. The dominant negative effect may be related to the inhibition of the nuclear-to-cytosol translation of VCP under MG132 treatment.

A recent study concluded that aggresome is important in LB formation [10], based on three reasons. The first is that LB consists of various proteins involved in the ubiquitin-proteasome system such as ubiquitinated proteins, proteasome subunits, parkin, α-synuclein, synphillin-1, Hsp70, and Hsp40 [11,17–19]. The second is the perinuclear localization, which is similar to LBs [2,10]. The third is the morphological similarity in the halo and core structures of LBs. The finding that VCP contributes to aggresome formation may enhance our understanding of the biogenesis of LBs.

References

[1] Forno, L.S. (1996) Neuropathology of Parkinson's disease. J. Neuropathol. Exp. Neurol. 55, 259–272.
[2] McNaught, K.S., Shashidharan, P., Perl, D.P., Jenner, P. and Olanow, C.W. (2002) Aggresome-related biogenesis of Lewy bodies. Eur. J. Neurosci. 16, 2136–2148.
[3] Johnston, J.A., Cristina, L.W. and Kopito, R.R. (1998) Aggresome: a cellular response to misfolded proteins. J. Cell. Biol. 143, 1883–1898.
[4] Mayer, R.J., Lowe, J., Lennox, G., Doherty, F. and Landon, M. (1989) Intermediate filaments and ubiquitin: a new thread in the understanding of chronic neurodegenerative diseases. Prog. Clin. Biol. Res. 317, 809–818.
[5] Neuwald, A.F., Aravind, L. and Koonin, E.V. (1999) AAA+: a class of chaperone-like ATPases associated with the assembly, operation and disassembly of protein complexes. Genome Res. 9, 27–43.
[6] Wang, Q., Song, C. and Li, C.C. (2004) Molecular perspectives on p97-VCP: progress in understanding its structure and diverse biological functions. J. Struct. Biol. 146, 44–57.
[7] Taylor, J.P., Tanaka, F., Robitschek, J., Sandoval, C.M., Taye, A., Markovic, P.S. and Fischbeck, K.H. (2003) Aggresomes protect cells by enhancing the degeneration of toxic polyglutamine-containing protein. Hum. Mol. Genet. 12, 749–757.
[8] Hirabayashi, M., Inoue, K., Tanaka, K., Nakadate, K., Ohsawa, Y., Kamei, Y., Popiel, A.H., Sinohara, A., Iwamatsu, A., Kimura, Y., Uchiyama, Y., Hori, S. and Kakizuka, A. (2001) VCP/P97 in abnormal protein aggregates, cytoplasmic vacuoles, and cell death, phenotypes relevant to neurodegeneration. Cell Death Differ. 8, 977–984.
[9] Mizuno, Y., Hori, S., Kakizuka, A. and Okamoto, K. (2003) Vacuole-creating protein in neurodegenerative diseases in humans. Neurosci. Lett. 343, 77–80.
[10] Olanow, C.W., Perl, D.P., DeMartino, G.N. and McNaught, K.S. (2004) Lewy-body formation is an aggresome-related process: a hypothesis. Lancet Neurol. 3, 496–503.
[11] Garcia-Mata, R., Gao, Y.S. and Sztul, E. (2002) Hassle with taking out the garbage: aggravating aggresomes. Traffic 3, 388–396.
[12] Dai, R.M., Chen, E., Long, D.L., Gorbae, C.M. and Li, C.C. (1998) Involvement of valosin-containing protein, an ATPase co-purified with IκBα and 26S proteasome, in ubiquitin-proteasome-mediated degradation of IκBα. J. Biol. Chem. 273, 3562–3573.
[13] Kobayashi, T., Tanaka, K., Inoue, K. and Kakizuka, A. (2002) Functional ATPase activity of p97/valosin-containing protein (VCP) is required for the quality control of endoplasmic reticulum in neuronally differentiated mammalian PC12 cells. J. Biol. Chem. 277, 47358–47365.
[14] Wang, Q., Song, C. and Li, C.C. (2003) Hexamerization of p97-VCP is promoted by ATP binding to the D1 domain and required for ATPase and biological activities. Biochem. Biophys. Res. Commun. 300, 253–260.

[15] Kopito, R.R. (2000) Aggresomes, inclusion bodies and protein aggregation. Trends Cell Biol. 10, 524–530.
[16] Johnston, J.A., Illing, M.E. and Kopito, R.R. (2002) Cytoplasmic dynin/dynactin mediates the assembly of aggresomes. Cell Motil. Cytoskeleton 53, 26–38.
[17] Muqit, M.M., Davidson, S.M., Payne Smith, M.D., MacCormac, L.P., Kahns, S., Jensen, P.H., Wood, N.W. and Latchman, D.S. (2004) Parkin in recruited into aggresomes in a stress-specific manner: over-expression of parkin reduces aggresome formation but can be dissociated from parkin's effect on neuronal survival. Hum. Mol. Genet. 13, 117–135.
[18] Tanaka, M., Kim, Y.M., Lee, G., Junn, E., Iwatsubo, T. and Mouradian, M.M. (2004) Aggresomes formed by α-synuclein and synphilin-1 are cytoprotective. J. Biol. Chem. 279, 4625–4631.
[19] Dul, J.L., Davu, D.P., Williamson, E.K., Stevens, F.J. and Argon, Y. (2001) Hsp70 and antifibrillogenic peptides promote degradation and inhibit intracellular aggregation of amyloidogenic light chains. J. Cell Biol. 152, 705–716.

Clinical Heterogeneity of α-Synuclein Gene Duplication in Parkinson's Disease

Kenya Nishioka, MD,[1] Shin Hayashi, MD,[2] Matthew J. Farrer, PhD,[3] Andrew B. Singleton, PhD,[4] Hiroyo Yoshino, BS,[5] Hisamasa Imai, MD,[6] Toshiaki Kitami, MD,[1] Kenichi Sato, MD,[1] Ryu Kuroda, MD,[7] Hiroyuki Tomiyama, MD,[1,7] Koichi Mizoguchi, MD,[7] Miho Murata, MD,[8,9] Tatsushi Toda, MD,[9,10] Issei Imoto, MD, PhD,[2] Johji Inazawa, MD, PhD,[2] Yoshikuni Mizuno, MD,[1,5] and Nobutaka Hattori, MD, PhD[1,5,9]

Objective: **Recently, genomic multiplications of α-synuclein gene (*SNCA*) have been reported to cause hereditary early-onset parkinsonism. The objective of this study was to assess the frequency of SNCA multiplications among autosomal dominant hereditary Parkinson's disease (ADPD).** ***Methods:*** **We screened 113 ADPD probands and 200 sporadic PD cases by quantitative polymerase chain reaction and confirmed *SNCA* multiplications by flurorescence in situ hybridization (FISH) and comparative genomic hybridization array.** ***Results:*** **Two families (two patients from Family A and one from Family B) with SNCA duplication were identified among ADPD patients. Even though they had the same *SNCA* duplication, one patient had dementia. Because there was exactly the same difference between the regions originated from each patient, the finding suggests that the phenotype of *SNCA* multiplication may be also influenced by the range of duplication region. We also detected asymptomatic carriers in the families of both patients. Interestingly, the penetrance ratio was 33.3% (2/6) in one kindred, indicating that the ratio was very much lower than expected.** ***Interpretation:*** **These two newly identified Japanese patients with *SNCA* duplication and the five previously identified American and European families with *SNCA* triplication or duplication mutations indicate that the incidence of *SNCA* multiplication may be more frequent than previously estimated.**

Ann Neurol 2006;59:298–309

Parkinson's disease (PD) is the second most common neurodegenerative disorder next to Alzheimer's disease (AD). Although the exact cause for PD remains to be elucidated, genetic factors could contribute to the pathogenesis of PD. Indeed, six causative genes and four chromosomal loci for familial PD (FPD) have been identified.[1–13] *α-Synuclein*, *UCH-L1*, and *LRRK2* have been identified as causative genes for autosomal dominant forms of FPD (ADPD), whereas *parkin*, *PINK1*, and *DJ-1* have been identified as causative genes for autosomal recessive forms of FPD (ARPD).[1,10,14] The presence of several causative genes and loci for FPD indicates that the pathogenic mechanisms of sporadic PD are also multifactorial. Studies of FPD are important as they enhance our understanding of nigral neuronal death. Furthermore, it has been proposed that the gene products for FPD are components of common pathways in sporadic PD. As testament, missense mutations such as A30P,[15] E46K,[16] and A53T,[9] in the N-terminal of α-synuclein gene (*SNCA*) have been linked to a rare form of FPD, and α-synuclein subsequently was confirmed to be a major component of Lewy bodies (LBs) and Lewy neurites, the pathological hallmark of sporadic PD and dementia with LBs (DLB).[17] Based on large population-based studies, missense mutations of *SNCA* are infrequent.[18] In particular, the SNCA A53T mutations identified in patients with FPD originate from a single founder. To date, SNCA A30P and E46K mutations have been found in only one family each, suggesting that missense mutations are a very rare cause of parkinsonism. Recently, *SNCA* multiplications in FPD haves been re-

From the [1]Department of Neurology, Juntendo University School of Medicine, Tokyo, Japan; [2]Department of Molecular Cytogenetics, Medical Research Institute and Graduate School of Biomedical Science, Tokyo Medical and Dental University, Tokyo, Japan; [3]Department of Neuroscience, Mayo Clinic, Jacksonville, FL; [4]Laboratory of Neurogenetics, National Institute on Aging, Neurogenetics Branch, National Institute of Neurological Disorders and Stroke, Genetic Diseases Research Branch, National Institute of Health, Bethesda, MD; [5]Research Institute for Disease of Old Ages, Juntendo University School of Medicine; [6]Deparment of Neurology, Tokyo Rinkai Hospital, Tokyo; [7]Department of Neurology, Shizuoka Institute of Epilepsy and Neurological Disorders, Shizuoka; [8]Department of Neurology, Musashi Hospital, National Center of Neurology and Psychiatry, Kodaira; [9]CREST, Japan Science and Technology Corporation, Kawaguchi, Saitama; and [10]Division of Functional Genomics, Osaka University Graduate School of Medicine, Suita, Japan.

Received Aug 10, 2005, and in revised form Oct 19. Accepted for publication Oct 22, 2005.

Published online December 15, 2005 in Wiley InterScience (www.interscience.wiley.com). DOI: 10.1002/ana.20753

Address correspondence to Dr Hattori, Department of Neurology, Juntendo University School of Medicine, 2-1-1 Hongo, Bunkyo, Tokyo 113-8421, Japan. E-mail: nhattori@med.juntendo.ac.jp

ported in two families with genomic triplication and in three families with duplications.[11–13,19] These findings suggest that overproduction of α-synuclein is one of the most important factors in FPD. In general, unequal intrachromosomal crossovers that result from misalignment of two homologous flanking sequences may account for genomic multiplications as well as deletions. The *SNCA* multiplications mutations, triplications, and duplications found in five unrelated patients probands with FPD are de novo within each kindred.[11–13,19] Affected individuals within the Iowa kindred, with *SNCA* genomic triplication, have fulminant, early-onset disease with a phenotype ranging clinically and pathologically from PD to diffuse LB disease (DLBD).[20] In contrast, *SNCA* duplication families have later onset disease and a longer duration to death, and neither cognitive decline nor dementia are prominent. Therefore, overproduction of wild-type α-synuclein (*SNCA*) may result in phenotypes of PD, PD with dementia (PDD), and DLBD, suggesting that regulation of α-synuclein protein levels is central to the cause of these phenotypes. In summary, the phenotype may be dependent on copy numbers of *SNCA*.

In this study, to gain further insight into the role of this multiplication, we assessed a series of 113 PD patients with autosomal dominant mode of inheritance and 200 sporadic PD patients for multiplication at this locus.

Subjects and Methods

Patients

This study consisted of 113 patients with ADPD and 200 patients with sporadic PD. Diagnosis of PD was adopted by the participating neurologists and the diagnosis was established based on the United Kingdom Parkinson's Disease Society Brain Bank criteria.[21] The mean age at onset of the 56 male and 57 female index patients with ADPD was 66.0 ± 9.5 (±SD), and that of the 81 male and 119 female patients with sporadic PD was 64.7 ± 10.0 (±SD). All patients were of Japanese origin. The study was approved by the ethics review committee of Juntendo University. Blood samples for genetic analysis were collected after obtaining informed consent from each patient and 17 unaffected relatives. None had mutations in *parkin*, *PINK1*, or *DJ-1*. We could not detect heterozygous exon deletions of such recessive genes by quantitative analysis in the patients studied. In addition, none had mutations in exon 41 in *LRRK2*.

Gene Dosage Analysis for SNCA

DNA was prepared using standard methods. The mutation screening was performed as described previously.[22] Semiquantitative multiplex polymerase chain reaction (PCR) of genomic DNA samples was performed using a real-time PCR method to detect the dosage of *SNCA* (ABI Prism 7700 sequence detector; Applied Biosystems, Foster City, CA). As the first step, we targeted exon 3 of *SNCA* to screen the gene dosage of *SNCA*. β-*Globin* gene was amplified as an endogenous reference. In addition, we used a DNA sample from the Iowa family (patients had triplication of *SNCA*) as a positive control. The primer and TaqMan MGB probe sequences used in this study are described in Table 1. PCR was conformed with PCR universal master mix using 25ng of genomic DNA, 900nM primers, and 250nM probes (β-globin is 50–200nM) in a total reaction volume of 50μL. PCR cycling conditions were 95°C for 10 minutes, 95°C for 15 seconds, and 60°C for 1 minute (40 cycles). Values between 0.4 and 0.6 were considered as heterozygous deletion, between 0.8 and 1.2 as normal, between 1.3 and 1.7 as heterozygous duplication, and greater than 1.8 as triplication.

In the second step, we performed semiquantitative analysis on exons 1/2, 4, 6, and 7 for the patients found to carry multiplication of this gene in the first step. All the sequences of this gene are shown in Table 1.

Fluorescence In Situ Hybridization Analysis

We used two-color standard fluorescence in situ hybridization (FISH) and prophase FISH for metaphase and interphase. FISH analyses were performed as described previously,[23] using a BAC located around the region of interest. The location of each bacterial artificial chromosome (BAC) was archived by the database of UCSC (http://genome.ucsc.edu) or NCBI (http://www.ncbi.nlm.nih.gov). Two BAC contigs representing the region at 4q21-22. BACs RP11-17p8 and RP11-61407 were used as probes. BAC RP11-17p8 locates at site of centromere of chromosome 4, and BAC RP11-61407 locates at site of telomere of the same chromosome. PR11-61407 contains *SNCA*, suggesting that the signal of this clone shows the copy numbers of *SNCA*. The distance between the two BAC clones was approximately 1.4Mb. Probes were labeled with biotin-16-dUTP or digoxigenin-11-dUTP by nick-translation (Roche Diagnostics, Tokyo, Japan). The copy number of the region was assessed according to the hybridization patterns observed on both metaphase and interphase chromosomes. We established Epstein–Barr virus (EBV)–transformed lymphoblastoid cell line as described previously.[24]

Multiplication (duplication) Region Using Comparative Genomic Hybridization Array and Gene Dosage Technique

The triplication region in Iowa family is between 1.61 and 2.04Mb and contains 17 annotated or putative genes. A recently constructed high-density comparative genomic hybridization (CGH) array, designated MCG Whole Genome Array-4500,[25] which contains 4532 BAC/P1-artificial chromosome (PAC) clones covering the entire genome at intervals of approximately 0.7Mb, was used for CGH array analysis. This array is suitable for detecting the size of the multiplication if the size is greater than 0.7Mb. Hybridizations were performed as described previously with minor modifications.[26,27] In brief, test and reference genomic DNAs from the patient's lymphoblastoid cells and normal lymphocytes, respectively, were labeled with Cy3- and Cy5-dCTP (Amersham Biosciences, Tokyo), respectively, precipitated together with ethanol in the presence of Cot-1 DNA, redissolved in a hybridization mix (50% formamide, 10% dextran sulfate, 2 × standard saline citrate [SSC], and 4% sodium dodecyl sulfate [SDS], pH 7.0),